Self-Assembled Chloro-Bridged (Arene)ruthenium Metallo-Prisms: Synthesis and Molecular Structure of Cationic Complexes of the Type $[Ru_6(\eta^6\text{-arene})_6(\mu_3\text{-tpt-}\kappa N)_2(\mu\text{-Cl})_6]^{6+}$ (tpt = 2,4,6-tris(pyridinyl)-1,3,5-triazine)

Padavattan Govindaswamy, Georg Süss-Fink, and Bruno Therrien*

Institut de Chimie, Université de Neuchâtel, Case postale 158, CH-2009 Neuchâtel, Switzerland

Received September 14, 2006

Cationic (arene)ruthenium-based hexanuclear complexes with trigonal-prismatic structures have been synthesized in good yield by self-assembly of only two components: the dinuclear (arene)ruthenium complexes $[Ru(\eta^6\text{-arene})(\mu\text{-Cl})Cl]_2$ (arene = *p*-$Pr^iC_6H_4Me$, C_6Me_6) react in water with 2,4,6-tris(pyridinyl)-1,3,5-triazine (tpt) derivatives in the presence of AgO_3SCF_3 to form hexanuclear cations of the general formula $[Ru_6(\eta^6\text{-arene})_6(\mu_3\text{-tpt-}\kappa N)_2(\mu\text{-Cl})_6]^{6+}$. In the presence of 2,4,6-tris(pyridin-4-yl)-1,3,5-triazine (4-tpt) the prismatic cations $[Ru_6(\eta^6\text{-}p\text{-}Pr^iC_6H_4Me)_6(\mu_3\text{-4-tpt-}\kappa N)_2(\mu\text{-Cl})_6]^{6+}$ (**3**) and $[Ru_6(\eta^6\text{-}C_6Me_6)_6(\mu_3\text{-4-tpt-}\kappa N)_2(\mu\text{-Cl})_6]^{6+}$ (**4**) have been isolated as the triflate salts, whereas with 2,4,6-tris(pyridin-3-yl)-1,3,5-triazine (3-tpt) $[Ru_6(\eta^6\text{-}p\text{-}Pr^iC_6H_4Me)_6(\mu_3\text{-3-tpt-}\kappa N)_2(\mu\text{-Cl})_6]^{6+}$ (**7**) and $[Ru_6(\eta^6\text{-}C_6Me_6)_6(\mu_3\text{-3-tpt-}\kappa N)_2(\mu\text{-Cl})_6]^{6+}$ (**8**) have been obtained and isolated as the triflate salts. In all cases, the neutral intermediates initially formed prior to the addition of silver triflate have been isolated and characterized as well: $[Ru_3(\eta^6\text{-}p\text{-}Pr^iC_6H_4Me)_3(\mu_3\text{-4-tpt-}\kappa N)Cl_6]$ (**1**), $[Ru_3(\eta^6\text{-}C_6Me_6)_3(\mu_3\text{-4-tpt-}\kappa N)Cl_6]$ (**2**), $[Ru_3(\eta^6\text{-}p\text{-}Pr^iC_6H_4Me)_3(\mu_3\text{-3-tpt-}\kappa N)Cl_6]$ (**5**), and $[Ru_3(\eta^6\text{-}C_6Me_6)_3(\mu_3\text{-3-tpt-}\kappa N)Cl_6]$ (**6**), respectively. In the case of a trigonal-prismatic hexacation containing *p*-cymene and 3-tpt ligands, the NMR spectra reveal a mixture of the two isomers **7a** and **7b**, the formation of which can be rationalized by molecular modeling. The single-crystal structure analyses of $[Ru_6(\eta^6\text{-}p\text{-}Pr^iC_6H_4Me)_6(\mu_3\text{-4-tpt-}\kappa N)_2(\mu\text{-Cl})_6][O_3SCF_3]_6$ ([**3**][O_3SCF_3]$_6$), $[Ru_6(\eta^6\text{-}C_6Me_6)_6(\mu_3\text{-4-tpt-}\kappa N)_2(\mu\text{-Cl})_6][O_3SCF_3]_6$ ([**4**][O_3SCF_3]$_6$), and $[Ru_6(\eta^6\text{-}C_6Me_6)_6(\mu_3\text{-3-tpt-}\kappa N)_2(\mu\text{-Cl})_6][O_3SCF_3]_6$ ([**8**][O_3SCF_3]$_6$) reveal strong π stacking interactions between the two tpt subunits of the trigonal prisms.

Introduction

Self-assembly of supramolecular architectures with transition-metal complexes is mainly dominated by square-planar metal coordination geometries. Pioneered by Fujita in 1990[1] and exploited by other groups,[2] the combination of 90° coordination building blocks and linear ligands to form square and rectangular networks has been extensively studied. A few years later, the same approach was used to generate three-dimensional networks.[3] So far, a multitude of two- and three-dimensional structures incorporating transition metals with square-planar geometry have been synthesized.[4] In the search for new building blocks for the synthesis of supramolecular materials with interesting properties, there is an increasing interest in using transition-metal complexes with octahedral geometry.[5] However, it is essential to control the directional bonding, since the metal center possesses six coordination sites. Cotton and co-workers have built up two- and three-dimensional architectures from metal−metal paddlewheel units such as $[Mo_2(\mu\text{-DAniF-}\kappa N,N')_3(CH_3CN)_2]^+$ (DAniF = *N*,*N*′-di-*p*-anisylformamidinate).[6] Similarly, the *fac*-$Re(CO)_3$ corner system was judiciously chosen to prepare molecular rectangles[7] or triangular prisms.[8] The triden-

* To whom correspondence should be addressed. E-mail: bruno.therrien@unine.ch.

(1) Fujita, M.; Yazaki, J.; Ogura, K. *J. Am. Chem. Soc.* **1990**, *112*, 5645−5647.

(2) (a) Kuehl, C. J.; Huang, S. D.; Stang, P. J. *J. Am. Chem. Soc.*, **2001**, *123*, 9634−9641. (b) Moriuchi, T.; Miyaishi, M.; Hirai, T. *Angew. Chem., Int. Ed.* **2001**, *40*, 3042−3045. (c) Das, N.; Mukherjee, P. S.; Arif, A. M.; Stang, P. J. *J. Am. Chem. Soc.* **2003**, *125*, 13950−13951. (d) Mukherjee, P. S.; Das, N.; Kryschenko, Y. K.; Arif, A. M.; Stang, P. J. *J. Am. Chem. Soc.* **2004**, *126*, 2464−2473. (e) Caskey, D. C.; Shoemaker, R. K.; Michl, J. *Org. Lett.* **2004**, *6*, 2093−2096. (f) Yoshizawa, M.; Nagao, M.; Kumazawa, K.; Fujita, M. *J. Organomet. Chem.* **2005**, *690*, 5383−5388. (g) Kim, D.; Paek, J. H.; Jun, M.-J.; Lee, J. Y.; Kang, S. O.; Ko, J. *Inorg. Chem.* **2005**, *44*, 7886−7894.

(3) Fujita, M.; Oguro, D.; Miyazawa, M.; Oka, H.; Yamaguchi, K.; Ogura, K. *Nature* **1995**, *378*, 469−471.

(4) (a) Pirondini, L.; Bertolini, F.; Cantadori, B.; Ugozzoli, F.; Massera, C.; Dalcanale, E. *Proc. Natl. Acad. Sci. U.S.A.* **2002**, *99*, 4911−4915 and references therein. (b) Ovchinnikov, M. V.; Holliday, B. J.; Mirkin, C. A.; Zakharov, L. N.; Rheingold, A. L. *Proc. Natl. Acad. Sci. U.S.A.* **2002**, *99*, 4927−4931 and references therein. (c) Kuehl, C. J.; Kryschenko, Y. K.; Radhakrishnan, U.; Seidel, S. R.; Huang, S. D.; Stang, P. J. *Proc. Natl. Acad. Sci. U.S.A.* **2002**, *99*, 4932−4936 and references therein. (d) Kuehl, C. J.; Yamamoto, T.; Seidel, S. R.; Stang, P. J. *Org. Lett.* **2002**, *4*, 913−915. (e) Kryschenko, Y. K.; Seidel, S. R.; Muddiman, D. C.; Nepomuceno, A. I.; Stang, P. J. *J. Am. Chem. Soc.* **2003**, *125*, 9647−9652. (f) Crowley, J. D.; Goshe, A. J.; Bosnich, B. *Chem. Commun.* **2003**, 2824−2825. (g) Fujita, M.; Tominaga, M.; Hori, A.; Therrien, B. *Acc. Chem. Res.* **2005**, *38*, 369−378 and references therein. (h) Caskey, D. C.; Michl, J. *J. Org. Chem.* **2005**, *70*, 5442−5448. (i) Maurizot, V.; Yoshizawa, M.; Kawano, M.; Fujita, M. *Dalton Trans.* **2006**, 2750−2756.

(5) (a) Mukherjee, P. S.; Min, K. S.; Arif, A. M.; Stang, P. J. *Inorg. Chem.* **2004**, *43*, 6345−6350. (b) Mahmoudkhani, A. H.; Côté, A. P.; Shimizu, G. K. H. *Chem. Commun.* **2004**, 2678−2679.

(6) Cotton, F. A.; Lin, C.; Murillo, C. A. *Acc. Chem. Res.* **2001**, *34*, 759−771 and references therein.

(7) (a) Woessner, S. M.; Helms, J. B.; Shen, Y.; Sullivan, B. P. *Inorg. Chem.* **1998**, *37*, 5406−5407. (b) Rajendran, T.; Manimaran, B.; Lee, F.-Y.; Lee, G.-H.; Peng, S.-M.; Wang, C. M.; Lu, K.-L. *Inorg. Chem.* **2000**, *39*, 2016−2017. (c) Sun, S.-S.; Silva, A. S.; Brinn, I. M.; Lees, A. J. *Inorg. Chem.* **2000**, *39*, 1344−1345. (d) Rajendran, T.; Manimaran, B.; Lee, F.-Y.; Chen, P.-J.; Lin, S.-C.; Lee, G.-H.; Peng, S.-M.; Chen, Y.-J.; Lu, K.-L. *Dalton Trans.* **2001**, 3346−3351. (e) Sun, S.-S.; Lees, A. J. *Inorg. Chem.* **2001**, *40*, 3154−3160.

10.1021/om060843k CCC: $37.00
Publication on Web 01/06/2007

tate ligand 1,4,7-trithiacyclononane, which coordinates facially to ruthenium, was used to form a supramolecular cube.[9] The underlying strategy in those examples implies the blocking of several coordination sites at the metal centers, thus generating a preorganized arrangement before the formation of the supramolecular assembly.

In a similar manner, cyclopentadienyl or arene ligands can be used to control the accessibility of coordination sites of an octahedral metal center.[10] The use of these η^5 or η^6 ligands has advantages. (i) The aromatic ligand occupies three of the six coordination sites at the metal center, and the resulting coordination geometry is pseudo-tetrahedral, allowing a better control of the synthesis of two- or three-dimensional assemblies. (ii) The aromatic ligand allows different substituents which can enhance the solubility or add new properties to the molecular assembly.

We have been working with arene ruthenium complexes for many years,[11] and decided to use them as versatile building blocks in supramolecular chemistry. The triangular prism is the simplest three-dimensional construction, which involves only five building blocks: two triangular subunits, and three linear connecting units:

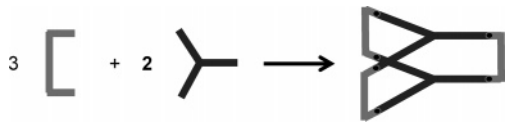

If these components do not contain stereogenic elements and if the two planar triangular subunits are perfectly eclipsed, the triangular prism obtained is achiral. However, a slight deviation from the eclipsed conformation generates a "double-rosette" type helicity with Δ or Λ configuration.[12] Recently we have shown the cationic triangular metallo-prisms $[Ru_6(\eta^6\text{-arene})_6(\mu_3\text{-4-tpt-}\kappa N)_2(\mu\text{-}C_2O_4\text{-}\kappa O)_3]^{6+}$ (arene = *p*-Pr^{i}C$_6$H$_4$Me, C$_6$Me$_6$) containing bridging oxalato ligands to have a double-helical chirality.[13] Using a similar approach, we have now synthesized chloro-bridged metallo-prisms connected by 2,4,6-tris(pyridin-4-yl)-1,3,5-triazine (4-tpt) and 2,4,6-tris(pyridin-3-yl)-1,3,5-triazine (3-tpt) ligands.

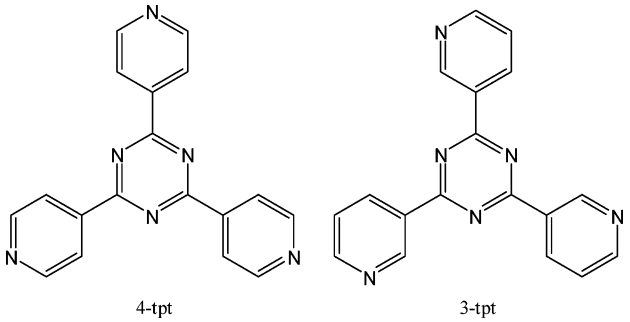

In this paper we report the synthesis and structural characterization of achiral cationic trigonal (arene)ruthenium metallo-prisms containing bridging chloro ligands.

Results and Discussion

The dinuclear (arene)ruthenium complexes $[Ru(\eta^6\text{-arene})(\mu\text{-Cl})Cl]_2$ (arene = *p*-Pr^{i}C$_6$H$_4$Me, C$_6$Me$_6$) and 2,4,6-tris(pyridin-4-yl)-1,3,5-triazine (4-tpt) react in water in the presence of AgO_3SCF_3 to form in low yield (<25%) the hexanuclear cations $[Ru_6(\eta^6\text{-}p\text{-Pr}^iC_6H_4Me)_6(\mu_3\text{-4-tpt-}\kappa N)_2(\mu\text{-Cl})_6]^{6+}$ (**3**) and $[Ru_6(\eta^6\text{-}C_6Me_6)_6(\mu_3\text{-4-tpt-}\kappa N)_2(\mu\text{-Cl})_6]^{6+}$ (**4**), respectively (see Scheme 1). However, we found that the yields of **3** and **4** can be increased significantly by isolating the neutral intermediates $[Ru_3(\eta^6\text{-}p\text{-Pr}^iC_6H_4Me)_3(\mu_3\text{-4-tpt-}\kappa N)Cl_6]$ (**1**) and $[Ru_3(\eta^6\text{-}C_6Me_6)_3(\mu_3\text{-4-tpt-}\kappa N)Cl_6]$ (**2**), followed by addition of silver triflate in dichloromethane, which affords **3** and **4** as the triflate salts in overall yields of about 65%. This significant improvement in the overall yield can be rationalized in terms of the tpt ligands being predisposed to form $\pi-\pi$ interacting systems, thus optimizing the formation of a prism over other assemblies. Despite a molecular weight of 3143.5 for $[\mathbf{3}][O_3SCF_3]_6$ and 3311.8 for $[\mathbf{4}][O_3SCF_3]_6$, the two hexanuclear complexes are quite soluble in $(CH_3)_2CO$, CH_3CN, and MeOH and sparingly soluble in CH_2Cl_2 and $CHCl_3$.

The ^{1}H NMR spectra of **1**−**4** display similar signal patterns for the pyridyl protons. Unlike the case for **1**, where H_α and H_β are found at the expected positions (9.3 and 8.5 ppm in CD_2Cl_2), in **3** the signals of H_α and H_β are almost superimposed at 8.7 ppm (see Figure 1). Upon formation of the triangular cationic prism **3**, the H_α signal is shifted upfield, whereas the H_β signal is shifted downfield. In **3**, the signals of the aromatic protons of the *p*-cymene ligand are shifted downfield as well as compared to those of **1** (Figure 1).

The infrared spectra of **1**−**4** are dominated by absorptions of the coordinated 2,4,6-tris(pyridin-4-yl)-1,3,5-triazine ligand, which are only slightly shifted as compared to those of the free ligand (1515 (s), 1374 (s), 794 (s), 641 (s) cm^{-1}).[14] In addition

(8) (a) Benkstein, K. D.; Hupp, J. T.; Stern, C. L. *J. Am. Chem. Soc.* **1998**, *120*, 12982−12983. (b) Benkstein, K. D.; Hupp, J. T. *Mol. Cryst. Liq. Cryst.* **2000**, *342*, 151−158. (c) Manimaran, B.; Rajendran, T.; Lu, Y.-L.; Lee, G.-H.; Peng, S.-M.; Lu, K.-L. *Eur. J. Inorg. Chem.* **2001**, 633−636. (d) Sun, S.-S.; Lees, A. J. *Chem. Commun.* **2001**, 103−104. (e) Manimaran, B.; Thanasekaran, P.; Rajendran, T.; Liao, R.-T.; Liu, Y.-H.; Lee, G.-H.; Peng, S.-M.; Rajagopal, S.; Lu, K.-L. *Inorg. Chem.* **2003**, *42*, 4795−4797.

(9) Roche, S.; Haslam, C.; Adams, H.; Heath, S. L.; Thomas, J. A. *Chem. Commun.* **1998**, 1681−1682.

(10) (a) Yan, H.; Süss-Fink, G.; Neels, A.; Stoeckli-Evans, H. *J. Chem. Soc., Dalton Trans.* **1997**, 4345−4350. (b) Piotrowski, H.; Hilt, G.; Schulz, A.; Mayer, P.; Polborn, K.; Severin, K. *Chem., Eur. J.* **2001**, *7*, 3196−3208. (c) Yamanari, K.; Ito, R.; Yamamoto, S.; Konno, T.; Fuyuhiro, A.; Fujioka, K.; Arakawa, R. *Inorg. Chem.* **2002**, *41*, 6824−6830. (d) Han, W. S.; Lee, S. W. *Dalton Trans.* **2004**, 1656−1663. (e) Wang, J.-Q.; Ren, C.-X.; Jin, G.-X. *Organometallics* **2006**, *25*, 74−81. (f) Zhang, Q.-F.; Adams, R. D.; Leung, W.-H. *Inorg. Chim. Acta* **2006**, *359*, 978−983.

(11) (a) Meister, G.; Rheinwald, G.; Stoeckli-Evans, H.; Süss-Fink, G. *J. Chem. Soc., Dalton Trans.* **1994**, 3215−3224. (b) Süss-Fink, G.; Plasseraud, L.; Ferrand, V.; Stanislas, S.; Neels, A.; Stoeckli-Evans, H.; Henry, M.; Laurenczy, G.; Roulet, R. *Polyhedron* **1998**, *17*, 2817−2827. (c) Fidalgo, E. G.; Plasseraud, L.; Suss-Fink, G. *J. Mol. Catal. A: Chem.* **1998**, *132*, 5−12. (d) Therrien, B.; Ward, T. R. *Angew. Chem., Int. Ed.* **1999**, *38*, 405−408. (e) Chérioux, F.; Therrien, B.; Süss-Fink, G. *Chem. Commun.* **2004**, 204−205. (f) Therrien, B.; Vieille-Petit, L.; Jeanneret-Gris, J.; Štěpnička, P.; Süss-Fink, G. *J. Organomet. Chem.* **2004**, *689*, 2456−2463. (g) Govindaswamy, P.; Yennawar, H. P.; Kollipara, M. R. *J. Organomet. Chem.* **2004**, *689*, 3108−3112. (h) Govindaswamy, P.; Carroll, P. J.; Mozharivskyj, Y. A.; Kollipara, M. R. *J. Organomet. Chem.* **2005**, *690*, 885−894. (i) Govindaswamy, P.; Mobin, S. M.; Thone, C.; Kollipara, M. R. *J. Organomet. Chem.* **2005**, *690*, 1218−1225.

(12) (a) Ikeda, A.; Udzu, H.; Zhong, Z.; Shinkai, S.; Sakamoto, S.; Yamaguchi, K. *J. Am. Chem. Soc.* **2001**, *123*, 3872−3877. (b) Prins, L. J.; Hulst, R.; Timmerman, P.; Reinhoudt, D. N. *Chem. Eur. J.* **2002**, *8*, 2288−2301. (c) Saalfrank, R. W.; Demleitner, B.; Glaser, H.; Maid, H.; Bathelt, D.; Hampel, F.; Bauer, W.; Teichert, M. *Chem. Eur. J.* **2002**, *8*, 2679−2683. (d) Fenniri, H.; Deng, B.-L.; Ribbe, A. E. *J. Am. Chem. Soc.* **2002**, *124*, 11064−11072. (e) Hiraoka, S.; Harano, K.; Tanaka, T.; Shiro, M.; Shionoya, M. *Angew. Chem., Int. Ed. Engl.* **2003**, *42*, 5182−5185. (f) ten Cate, M. G. J.; Omerović, M.; Oshovsky, G. V.; Crego-Calama, M.; Reinhoudt, D. N. *Org. Biomol. Chem.* **2005**, *3*, 3727−3733.

(13) Govindaswamy, P.; Linder, D.; Lacour, J.; Süss-Fink, G.; Therrien, B. *Chem. Commun.* **2006**, 4691−4693.

(14) Biedermann, H.-G.; Wichmann, K. *Z. Naturforsch.* **1974**, *29b*, 360−362.

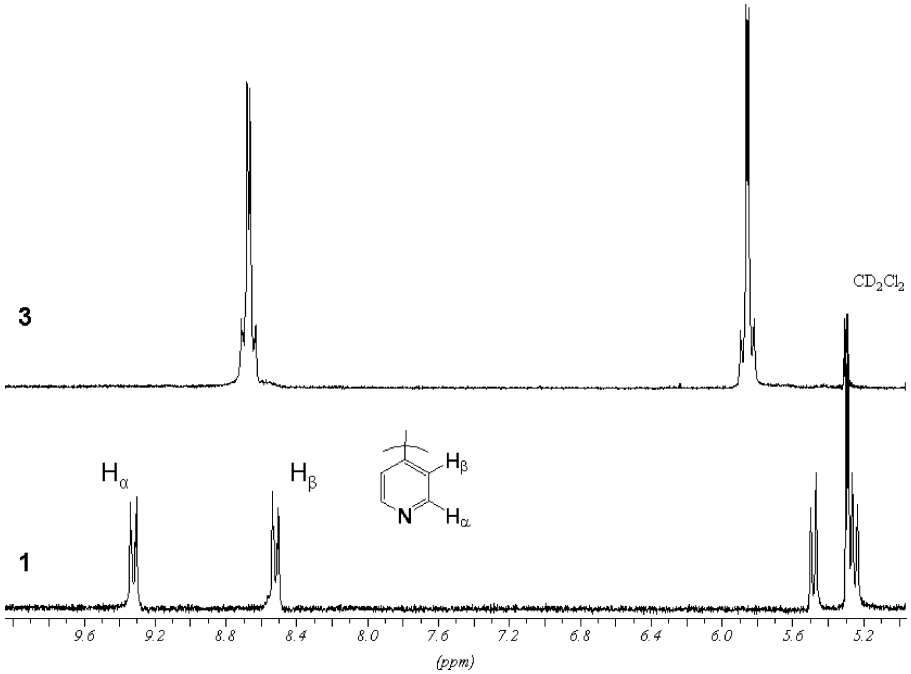

Figure 1. ^{1}H NMR spectra in CD_2Cl_2 of **1** (bottom) and **3** (top), showing the pyridyl region of the 2,4,6-tris(pyridin-4-yl)-1,3,5-triazine ligands and the aromatic region of the *p*-cymene ligands.

Scheme 1

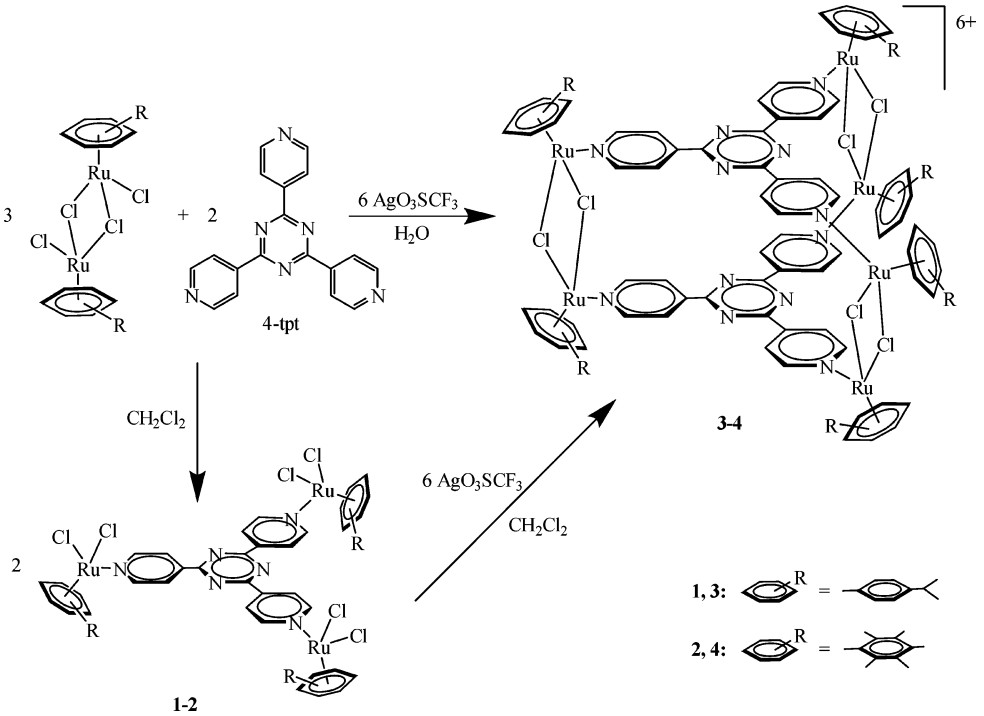

to the 4-tpt signals, strong absorptions attributed to the triflate anions (1260 (s), 1030 (s), 639 (s) cm^{-1})[15] are observed in the infrared spectra of [**3**][O_3SCF_3]$_6$ and [**4**][O_3SCF_3]$_6$.

The X-ray structure analyses of [**3**][O_3SCF_3]$_6$ and [**4**][O_3SCF_3]$_6$ show strong parallel π stacking interactions between the aromatic rings of the 4-tpt subunits (Figures 2 and 3). The centroid···centroid distances observed between corresponding aromatic rings of the $\pi-\pi$ interacting systems (3.42−3.64 Å) are shorter than the theoretical value calculated for this stacking mode[16] but comparable to the 3.46 Å separation observed between the triazine rings of two independent 4-tpt units in the crystal packing of [$Ir_3(\eta^5$-$C_5Me_5)_3(\mu_3$-4-tpt-$\kappa N)\{\eta^2$-$S_2C_2(B_{10}H_{10})$-$\kappa S\}_3$].[17] Interestingly, the two 4-tpt units are closer in **4**, despite the slightly longer Ru−Ru separations (**3**, 3.68 Å; **4**, 3.71 Å). However, these Ru−Ru distances are comparable to those found in the chloro-bridged dinuclear complexes [Ru(η^6-*p*-$Pr^iC_6H_4$-Me)(μ-Cl)Cl]$_2$ (3.69 Å)[18] and [Ru(η^6-C_6Me_6)(μ-Cl)Cl]$_2$ (3.743-(1) Å).[19] In the crystal packing of **3** and **4**, no π-stacking

(15) Johnston, D. H.; Shriver, D. F. *Inorg. Chem.* **1993**, *32*, 1045−1047.

(16) Tsuzuki, S.; Honda, K.; Uchimura, T.; Mikami, M.; Tanabe, K. *J. Am. Chem. Soc.* **2002**, *124*, 104−112.

(17) Wang, J.-Q.; Ren, C.-X.; Jin, G.-X. *Chem. Commun.* **2005,** 4738−4740.

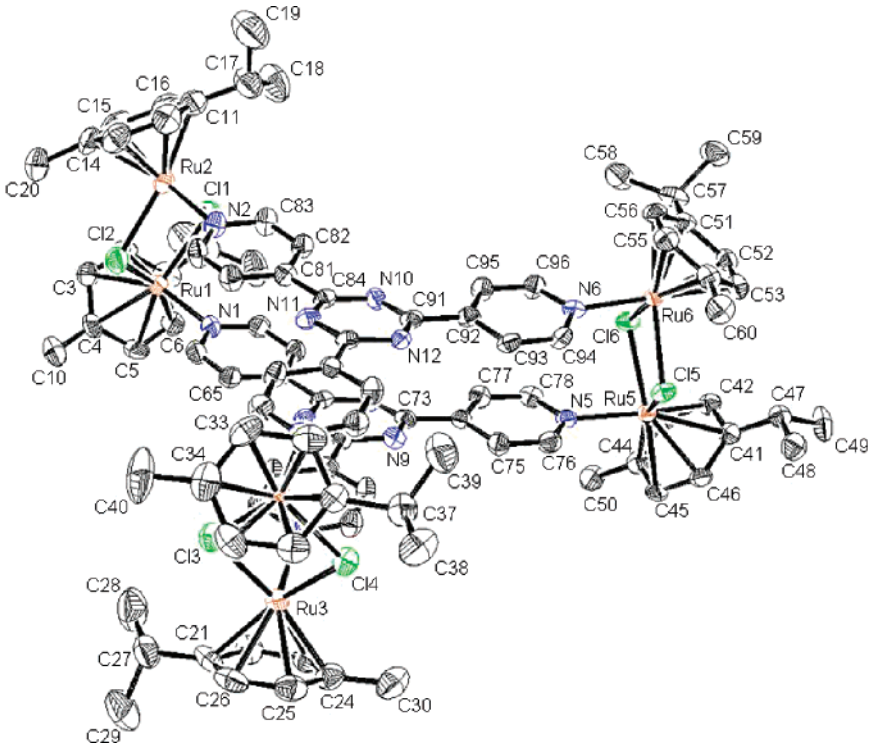

Figure 2. ORTEP drawing of cation **3** with the hydrogen atoms, acetone molecule, and O_3SCF_3 anions omitted for clarity.

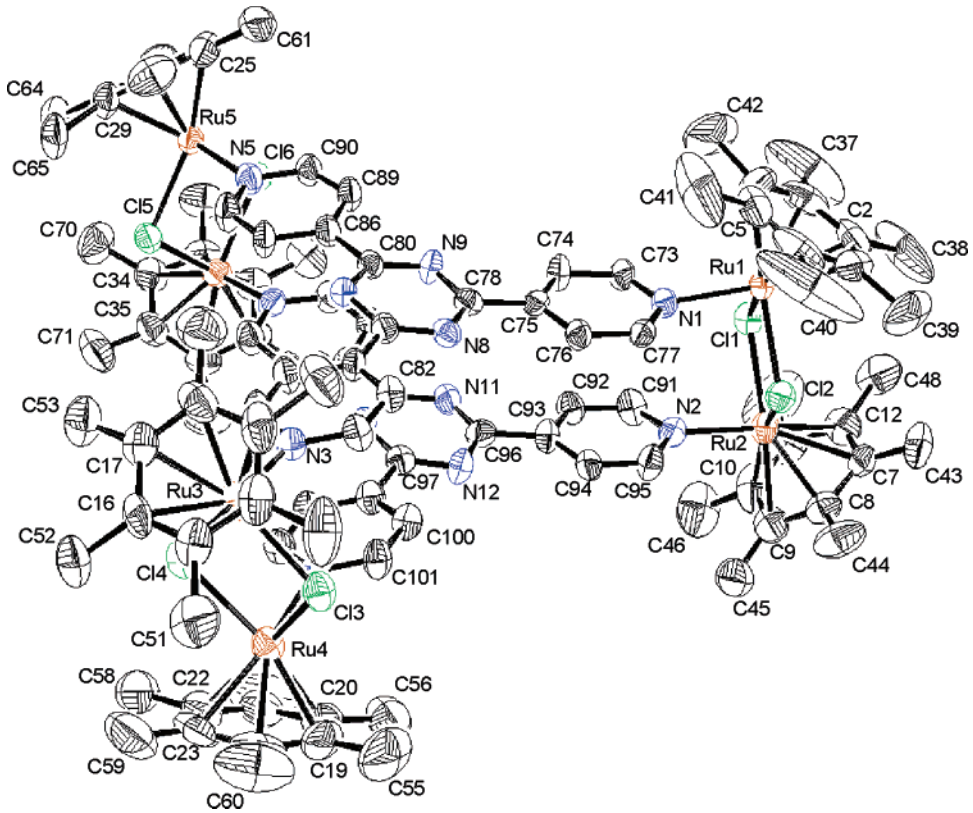

Figure 3. ORTEP drawing of cation **4** with the hydrogen atoms and O_3SCF_3 anions omitted for clarity.

interacting systems are observed between independent molecules. The empty spaces left between the cationic hexanuclear cations are filled with O_3SCF_3 anions (Figure 4). Selected bond lengths and angles are presented in Table 1.

The dinuclear arene ruthenium complexes $[Ru(\eta^6\text{-arene})(\mu\text{-}Cl)Cl]_2$ (arene = *p*-$Pr^iC_6H_4Me$, C_6Me_6) also react with 2,4,6-tris(pyridin-3-yl)-1,3,5-triazine (3-tpt) in dichloromethane to give in excellent yield the trinuclear complexes $[Ru_3(\eta^6\text{-}p\text{-}Pr^iC_6H_4Me)_3(\mu_3\text{-3-tpt-}\kappa N)Cl_6]$ (**5**) and $[Ru_3(\eta^6\text{-}C_6Me_6)_3(\mu_3\text{-3-tpt-}\kappa N)Cl_6]$ (**6**), respectively. Subsequent addition of silver triflate to **5** and **6** in dichloromethane affords the hexanuclear cationic prisms $[Ru_6(\eta^6\text{-}p\text{-}Pr^iC_6H_4Me)_6(\mu_3\text{-3-tpt-}\kappa N)_2(\mu\text{-}Cl)_6]^{6+}$ (**7**) and $[Ru_6(\eta^6\text{-}$

(18) Allardyce, C. S.; Dyson, P. J.; Ellis, D. J.; Salter, P. A.; Scopelliti, R. *J. Organomet. Chem.* **2003**, *668*, 35−42.
(19) McCormick, F. B.; Gleason, W. B. *Acta Crystallogr.* **1988**, *C44*, 603−605.

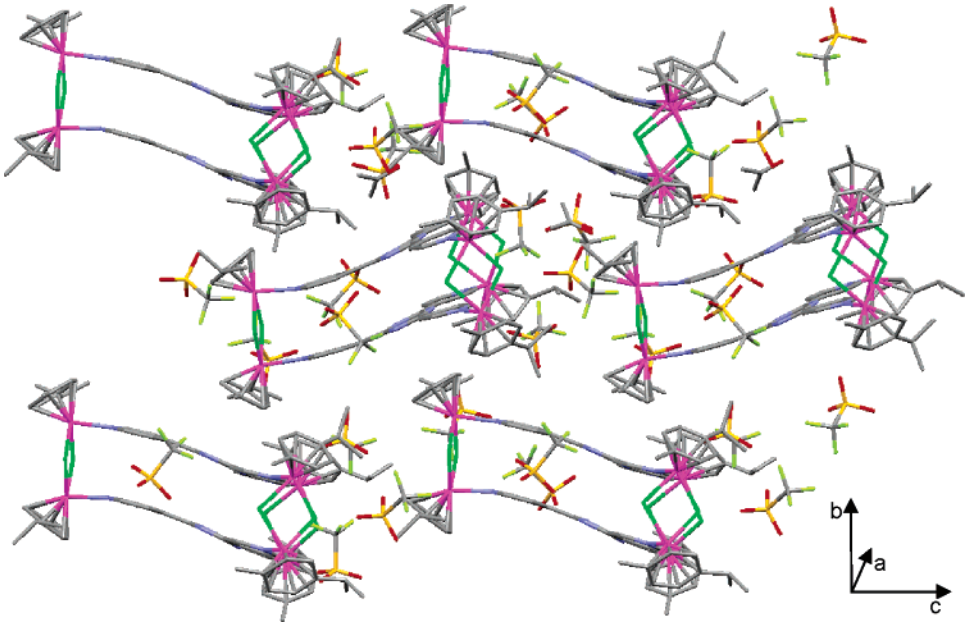

Figure 4. Crystal packing of [**3**][O_3SCF_3]$_6$·$(CH_3)_2CO$.

Scheme 2

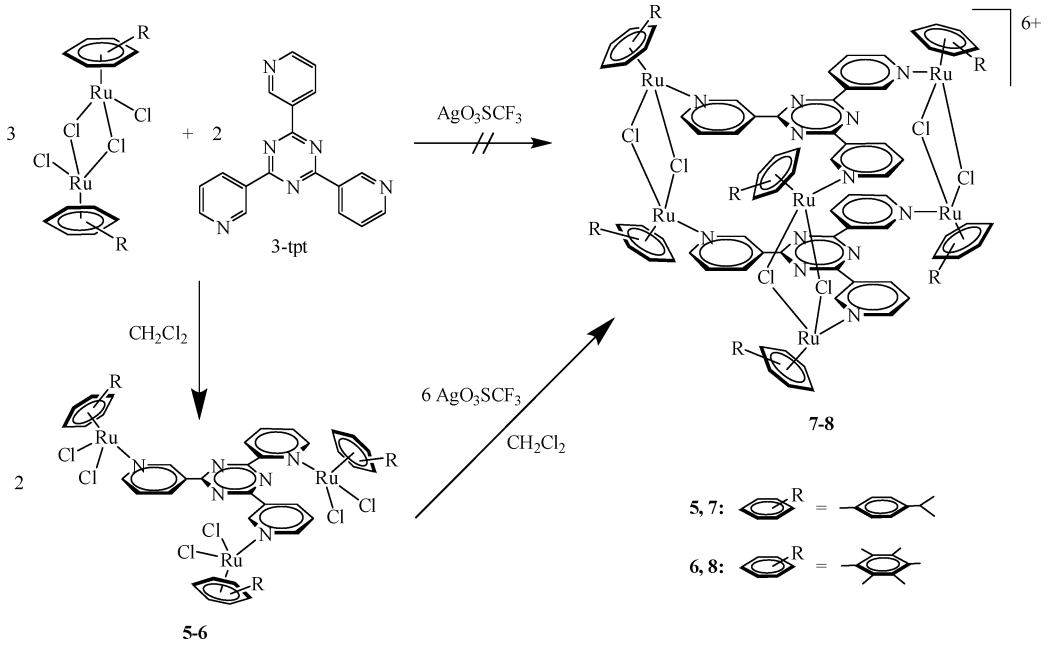

$C_6Me_6)_6(\mu_3$-3-tpt-$\kappa N)_2(\mu$-Cl)$_6]^{6+}$ (**8**), also isolated as their triflate salts (see Scheme 2). The direct reaction of [Ru(η^6-arene)(μ-Cl)Cl]$_2$ and 3-tpt in the presence of AgO_3SCF_3, however, does not afford **7** and **8**.[20]

The ^{1}H NMR spectrum of **8** shows, as expected, a well-organized structure with only one singlet for the methyl protons of the η^6-C_6Me_6 ligands and four signals for the four different pyridyl protons in the 3-tpt ligands. However, the ^{1}H NMR spectrum of **7** shows two sets of signals in an almost 1:1 ratio, one corresponding to the symmetrical isomer **7a**, in which all pyridyl and *p*-cymene moieties are equivalent, and a second one corresponding to the asymmetric isomer **7b**, containing three nonequivalent pyridyl and *p*-cymene groups (see Figure 5). Unable to obtain suitable crystals of **7a** or **7b** for an X-ray structure analysis, we determined the molecular structure of [**8**]-[O_3SCF_3]$_6$ (see Figure 6).

The molecular structure of [**8**][O_3SCF_3]$_6$ shows, as observed in [**3**][O_3SCF_3]$_6$ and [**4**][O_3SCF_3]$_6$, strong parallel π-stacking interactions between the aromatic rings of the tpt subunits. The centroid···centroid distances observed between corresponding aromatic rings of the $\pi-\pi$ interacting system (range 3.50−3.59 Å) are comparable to those found in cations **3** and **4**. Otherwise, all distances and angles are similar to those found in [**3**][O_3-SCF_3]$_6$ and [**4**][O_3SCF_3]$_6$ (see Table 1).

It is obvious from the space-filling representation of cation **8** (Figure 7) that two $Ru_2(\eta^6$-$C_6Me_6)_2(\mu$-$Cl)_2^{2+}$ connecting units cannot fit into the same trigonal segment. However, two Ru_2-$(\eta^6$-*p*-$Pr^iC_6H_4Me)_2(\mu$-$Cl)_2^{2+}$ connecting units can possibly be accommodated in the same segment, adopting a "face-to-face" conformation. To confirm this assumption, molecular modeling using the Hyperchem software was performed.

(20) A complex mixture of unidentified materials was obtained when the dinuclear (arene)ruthenium complexes [Ru(η^6-arene)(μ-Cl)Cl]$_2$ and 3-tpt were mixed in water in the presence of AgO_3SCF_3.

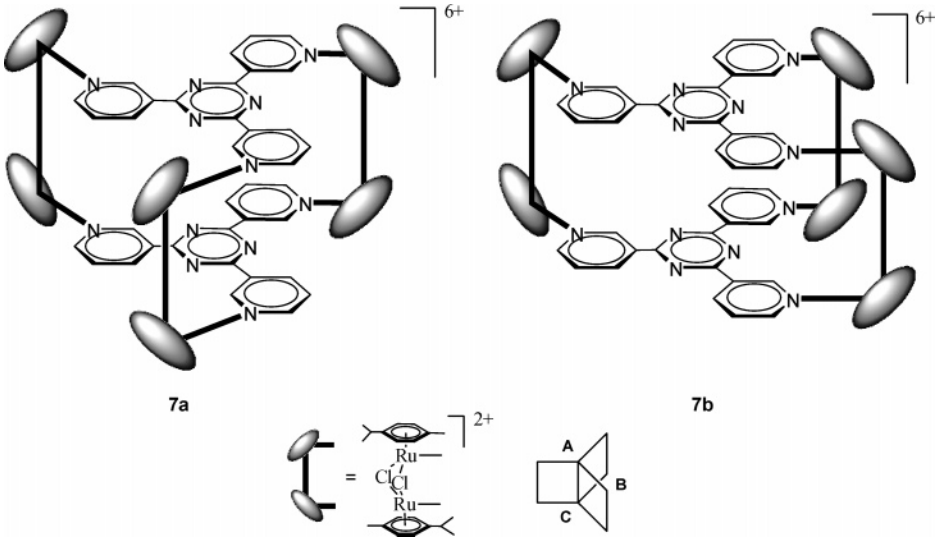

Figure 5. Schematic representations of the symmetrical isomer **7a** (left) and unsymmetrical isomer **7b** (right) with identification of the trigonal segments (**A**−**C**).

Table 1. Selected Bond Lengths and Angles for Cations 3, 4, and 8

	3	4	8
	Distances (Å)		
Ru(1)−N(1)	2.128(6)	2.127(4)	2.104(6)
Ru(2)−N(2)	2.123(6)	2.096(5)	2.114(6)
Ru(3)−N(3)	2.140(6)	2.121(4)	2.125(6)
Ru(4)−N(4)	2.122(6)	2.105(5)	2.111(5)
Ru(5)−N(5)	2.112(6)	2.110(4)	2.122(6)
Ru(6)−N(6)	2.122(6)	2.116(5)	2.113(6)
Ru(1)−Ru(2)	3.6649(8)	3.7263(8)	3.7214(9)
Ru(3)−Ru(4)	3.6783(7)	3.7060(9)	3.7085(9)
Ru(5)−Ru(6)	3.6871(7)	3.7417(8)	3.7025(9)
	Angles (deg)		
Ru(1)−Cl(1)−Ru(2)	97.75(7)	98.71(5)	99.07(6)
Ru(1)−Cl(2)−Ru(2)	97.62(7)	100.78(5)	98.44(6)
Ru(3)−Cl(3)−Ru(4)	98.36(6)	99.69(5)	98.56(6)
Ru(3)−Cl(4)−Ru(4)	98.04(6)	99.53(5)	98.58(7)
Ru(5)−Cl(5)−Ru(6)	98.52(7)	98.05(5)	99.01(6)
Ru(5)−Cl(6)−Ru(6)	98.41(7)	99.54(5)	97.37(6)

The model was built from the molecular structure of cation **8**, in which four methyl groups on each hexamethylbenzene ligand were removed and replaced by hydrogen atoms, giving rise to the hypothetical cations $[Ru_6(\eta^6\text{-}1,4\text{-}Me_2C_6H_4)_6(\mu_3\text{-}3\text{-}tpt\text{-}\kappa N)_2(\mu\text{-}Cl)_6]^{6+}$. From this model, which possesses steric constraint similar to that of the *p*-cymene derivative, one $Ru_2(\eta^6\text{-}1,4\text{-}Me_2C_6H_4)_2(\mu\text{-}Cl)_2(NC_5H_4)_2^{2+}$ connecting unit was rotated by 180° and reattached to the triazine cores, thus introducing a second dinuclear connecting unit in the same trigonal segment. The conformation was optimized by the Hyperchem software to give the expected unsymmetrical isomer (**7b**) without imposing unacceptable distortion on the 3-tpt ligands or around the diruthenium connecting units (see Figure 8).

On the basis of these findings, a more detailed NMR study of $[\mathbf{7}][O_3SCF_3]_6$ using standard 1D and 2D experiments was carried out, in order to confirm the molecular structures proposed for the two isomers **7a** and **7b**. As mentioned before, the ^{1}H NMR spectrum of **7** displays two distinct sets of signals, which is particularly obvious in the pyridyl region (see Figure 9). The first set of signals (▲), which shows chemical shifts similar to those of $[\mathbf{8}][O_3SCF_3]_6$, is assigned to the symmetrical structure (isomer **7a**). The second set of signals (●) is more complex: three different signals (δ 9.28, 9.23, and 8.88 ppm) can be identified by a COSY experiment as the H_γ pyridyl protons of the two 3-tpt ligands. The signal at δ 8.88 ppm is assigned to the H_γ atoms (of the two equivalent eclipsed pyridyl rings) in the trigonal segment **A** of the molecule **7b** (see Figure 5), while the two remaining signals of the H_γ atoms situated in segment **C** appear downfield at δ 9.28 and 9.23 ppm. The H_δ protons of the three pyridyl rings of two equivalent 3-tpt ligands give rise to two signals at δ 9.64 and 9.57 ppm (ratio 2:1), because the H_δ atoms, being in the same trigonal segment **B**, merge at δ 9.64 ppm, while the H_δ atoms in segment **A** are distinguishable. The H_α and H_β protons, situated at the periphery of the trigonal prism, appear as unresolved multiplets centered at 8.85 and 7.70 ppm, respectively.

In the aromatic region of the ^{1}H NMR spectrum of $[\mathbf{7}][O_3SCF_3]_6$ eight doublets of doublets are expected for the *p*-cymene protons, two for the symmetrical isomer **7a** and six for the unsymmetrical **7b**, but the aromatic resonances are all superimposed between δ 5.9 and 6.6 ppm. However, three well-separated septets for the CH of the isopropyl group of the *p*-cymene ligands are observed: one corresponding to **7a** and the remaining two, which show a 2:1 integration ratio, to isomer **7b**. Finally, instead of the expected four singlets for the methyl groups of the *p*-cymene ligands two badly resolved signals are observed at δ 2.49 and 2.35 ppm, while a pseudo-multiplet centered at δ 1.45 ppm is observed for the methyl protons of the isopropyl substituents, instead of the expected four doublets.

It is well-known that coordinating solvents can cleave chloro-bridged dinuclear (arene)ruthenium complexes.[21] In order to examine the stability of the chloro-bridged prisms **3**, **4**, **7**, and **8** in solution, we recorded the ^{1}H NMR spectra in various deuterated solvents (CD_2Cl_2, $(CD_3)_2CO$, CD_3CN) with different coordinating abilities. At room temperature and even elevated temperature, ^{1}H NMR experiments for **3**, **4**, **7**, and **8** in dichloromethane-d_2 and acetone-d_6 showed no signal changes, indicating the cleavage of the chloro bridges or the presence of free tpt units. However, in acetonitrile-d_3, all complexes show additional signals attributed to species generated by coordination of CD_3CN ligands, in line with cleavage of the chloro bridges.

In conclusion, we have opened a simple and straightforward access to chloro-bridged (arene)ruthenium metallo-prisms. These metallo-prisms show strong π stacking interactions between the

(21) (a) Bennett, M. A.; Smith, A. K. *J. Chem. Soc., Dalton Trans.* **1974**, 233−241. (b) Volland, M. A. O.; Hansen, S. M.; Rominger, F.; Hofmann, P. *Organometallics* **2004**, *23*, 800−816.

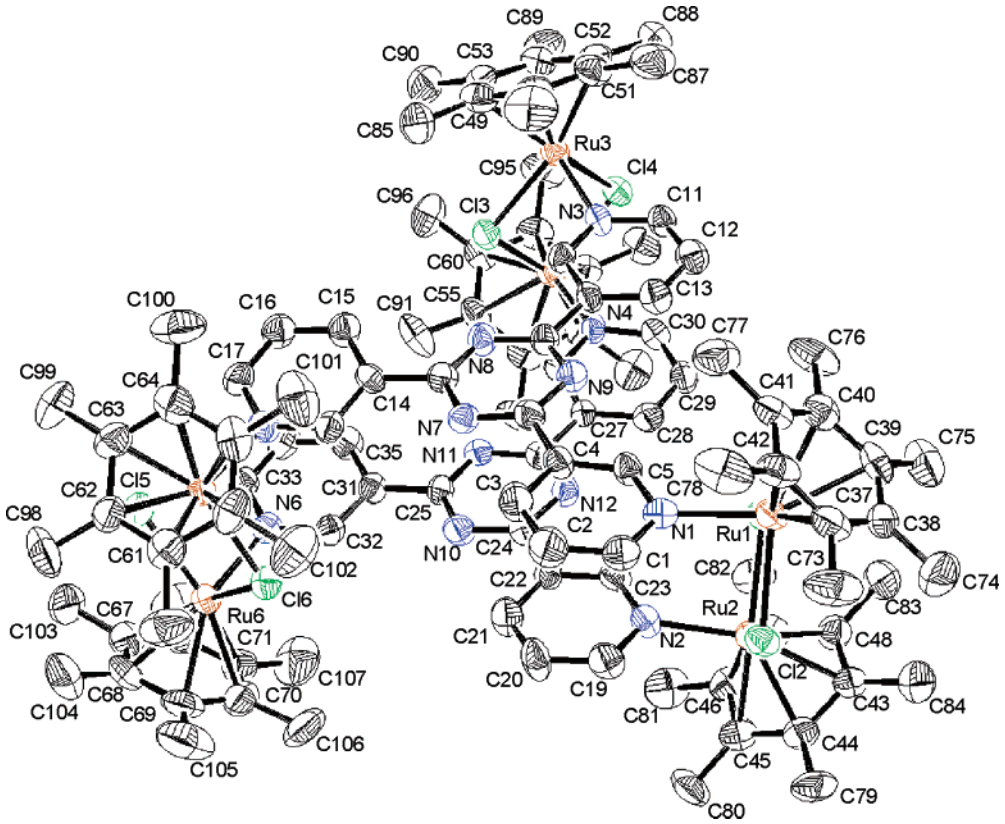

Figure 6. ORTEP drawing of cation **8** with the hydrogen atoms and O_3SCF_3 anions omitted for clarity.

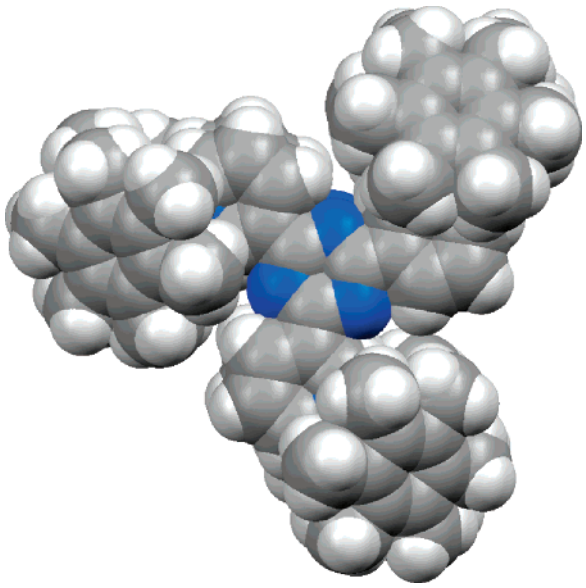

Figure 7. Space-filling representation of cation **8**.

tpt units, as demonstrated by ^{1}H NMR spectroscopy and X-ray structure analyses.

Experimental Section

General Remarks. [Ru(η^6-*p*-Pr^{i}C$_6$H$_4$Me)(μ-Cl)Cl]$_2$,[22] [Ru(η^6-C$_6$Me$_6$)(μ-Cl)Cl]$_2$,[23] 2,4,6-tris(pyridin-4-yl)-1,3,5-triazine, and 2,4,6-tris(pyridin-3-yl)-1,3,5-triazine[24] were prepared according to published methods. All other reagents were commercially available and were used as received. UV/visible absorption spectra were recorded on a Uvikon 930 spectrophotometer using precision cells made of quartz (1 cm) and exploited with Excel. The ^{1}H and ^{13}C{^{1}H} NMR spectra were recorded on a Varian Gemini 200 or Bruker AMX 400 spectrometer using the residual protonated solvent as internal standard. Infrared spectra were recorded as KBr pellets on a Perkin-Elmer FTIR 1720-X spectrometer. Microanalyses were performed by the Laboratory of Pharmaceutical Chemistry, University of Geneva, Geneva, Switzerland.

[Ru$_3$(η^6-*p*-Pr^{i}C$_6$H$_4$Me)$_3$(μ_3-4-tpt-κN)Cl$_6$] (1).[25] A mixture of [Ru(η^6-*p*-Pr^{i}C$_6$H$_4$Me)(μ-Cl)Cl]$_2$ (100 mg, 0.163 mmol) and 4-tpt (34 mg, 0.109 mmol) was suspended in CH_2Cl_2 (20 mL) and stirred for 3 h at 40 °C. The orange precipitate was filtered, washed with diethyl ether, and dried under vacuum (yield 130 mg, 97%). ^{1}H NMR (200 MHz, $CDCl_3$): δ (ppm) 9.43 (d, 6H, ^3J = 6.60 Hz, H$_\alpha$), 8.22 (d, 6H, H$_\beta$), 5.61 (d, 6H, ^3J = 5.86 Hz, Ar$_{p-cym}$), 5.41 (d, 6H, Ar$_{p-cym}$), 3.06 (sep, 3H, ^3J = 6.96 Hz, C*H*(CH$_3$)$_2$), 2.20 (s, 9H, CH$_3$), 1.39 (d, 18H, CH(C*H*$_3$)$_2$). IR (cm^{-1}): 1518 (s), 1371 (s), 806 (s). Anal. Calcd for $C_{48}H_{54}N_6Cl_6Ru_3$: C, 46.83; H, 4.42; N, 6.82. Found: C, 46.13; H, 4.24; N, 6.69.

[Ru$_3$(η^6-C$_6$Me$_6$)$_3$(μ_3-4-tpt-κN)Cl$_6$] (2). A mixture of [Ru(η^6-C$_6$Me$_6$)(μ-Cl)Cl]$_2$ (100 mg, 0.149 mmol) and 4-tpt (31.1 mg, 0.099 mmol) was suspended in CH_2Cl_2 (20 mL) and stirred for 3 h at 40 °C. The volume was reduced to 5 mL, and the orange-red solid was precipitated by addition of diethyl ether and filtered (yield 129 mg, 98%). ^{1}H NMR (400 MHz, $CDCl_3$): δ (ppm) 9.21 (d, 6H, ^3J = 5.60 Hz, H$_\alpha$), 8.42 (d, 6H, H$_\beta$), 2.09 (s, 54H, CH$_3$). ^{13}C{^{1}H} NMR (100 MHz, $CDCl_3$): δ (ppm) 171.0, 156.6, 143.0, 123.2, 92.1, 16.0. IR (cm^{-1}): 1516(s), 1371(s), 809(s). Anal. Calcd for $C_{54}H_{66}N_6Cl_6Ru_3$: C, 49.32; H, 5.06; N, 6.39. Found: C, 49.78; H, 5.04; N, 6.38.

[Ru$_6$(η^6-*p*-Pr^{i}C$_6$H$_4$Me)$_6$(μ_3-4-tpt-κN)$_2$(μ-Cl)$_6$][O$_3$SCF$_3$]$_6$ ([3][O$_3$SCF$_3$]$_6$). A mixture of **1** (100 mg, 0.0812 mmol) and Ag(O$_3$-

(22) Zelonka, R. A.; Baird, M. C. *Can. J. Chem.* **1972**, *50*, 3063−3072.
(23) Bennett, M. A.; Huang, T.-N.; Matheson, T. W.; Smith, A. K. *Inorganic Syntheses*; Wiley: New York, 1982; Vol. 21, p 74.
(24) Anderson, H. L.; Anderson, S.; Sanders, J. K. M. *J. Chem. Soc., Perkin Trans. 1* **1995**, 2231−2246.

(25) Due to solubility problems, no clear ^{13}C NMR spectrum could be obtained for **1**.

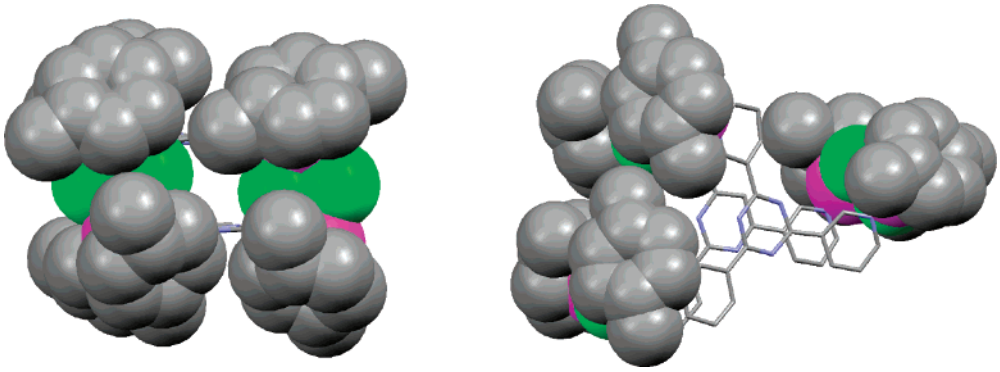

Figure 8. Molecular modeling of the unsymmetrical isomer (**7b**) using the Hyperchem software (two different orientations with mixed representation).

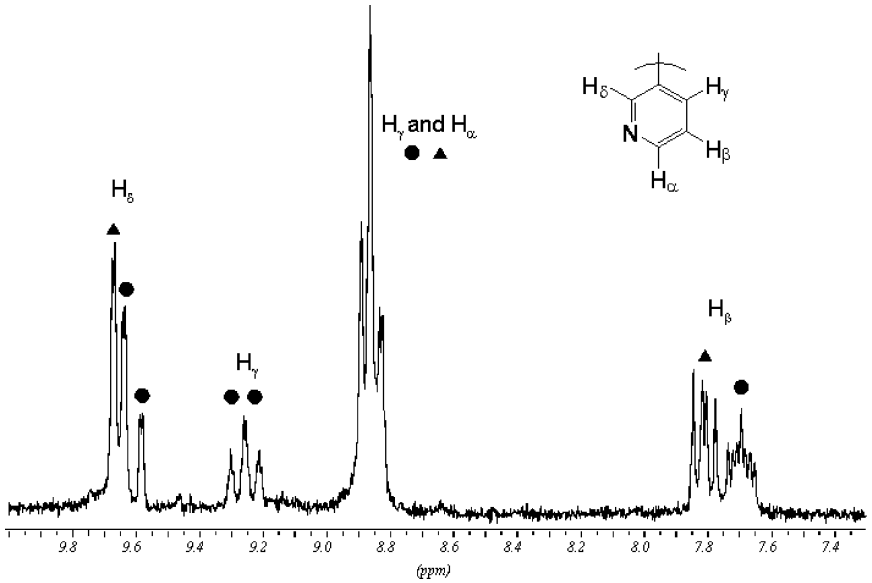

Figure 9. ^{1}H NMR (200 MHz, acetone-d_6) spectrum of cations **7a** (▲) and **7b** (●), showing the pyridyl region of the 2,4,6-tris(pyridin-3-yl)-1,3,5-triazine ligand.

SCF_3) (62.6 mg, 0.243 mmol) in CH_2Cl_2 (20 cm^3) was stirred at 50 °C for 4 h and then filtered. The filtrate was concentrated (3 mL), and diethyl ether was slowly added to precipitate an orange solid (yield 80 mg, 63%). ^{1}H NMR (400 MHz, acetone-d_6): δ (ppm) 8.83 (dd, 12H, ^3J = 6.80 Hz, ^4J = 1.16 Hz, H$_\alpha$), 8.79 (dd, 12H, H$_\beta$), 6.28 (d, 12H, ^3J = 6.60 Hz, Ar$_{p-cym}$), 6.17 (d, 12H, Ar$_{p-cym}$), 3.07 (sep, 6H, ^3J = 6.88 Hz, C*H*(CH$_3$)$_2$), 2.31 (s, 18H, C*H*$_3$), 1.46 (d, 36H, CH(C*H*$_3$)$_2$). ^{13}C{^{1}H} NMR (100 MHz, acetone-d_6): δ (ppm) 170.03, 156.41, 143.99, 125.38, 105.32, 100.56, 83.47 (d), 31.16, 21.85, 17.68. IR (cm^{-1}): 1520 (s), 1376 (s), 1260 (s), 1161 (s), 1030 (s), 810 (s), 639 (s). Anal. Calcd for $C_{102}H_{108}Cl_6F_{18}N_{12}O_{18}S_6Ru_6$: C, 38.97; H, 3.46; N, 5.34. Found: C, 38.83; H, 3.32; N, 5.08.

Crystals suitable for X-ray structure analyses were obtained by slow diffusion of diethyl ether in an acetone solution of [**3**][O_3SCF_3]$_6$.

[Ru$_6$(η^6-C$_6$Me$_6$)$_6$(μ_3-4-tpt-κN)$_2$(μ-Cl)$_6$][O$_3$SCF$_3$]$_6$ ([4][O$_3$SCF$_3$]$_6$). This compound was prepared by the same procedure described above for **3** using Ag(O_3SCF_3) (59 mg, 0.228 mmol) and **2** (100 mg, 0.076 mmol) (yield 82 mg, 65%). ^{1}H NMR (400 MHz, acetone-d_6): δ (ppm) 8.81 (dd, 12H, ^3J = 5.24 Hz, ^4J = 1.44 Hz, H$_\alpha$), 8.61 (dd, 12H, H$_\beta$), 2.18 (s, 108H, CH$_3$). ^{13}C{^{1}H} NMR (100 MHz, acetone-d_6): δ (ppm) 170.4, 156.1, 144.1, 126.0, 93.9, 15.3. IR (cm^{-1}): 1520 (s), 1383 (s), 1259 (s), 1160 (s), 1030 (s), 811 (s), 639 (s). Anal. Calcd for $C_{114}H_{132}N_{12}Cl_6O_{18}S_6F_{18}Ru_6$: C, 41.34; H, 4.01; N, 5.07. Found: C, 41.38; H, 3.99; N, 4.96.

Crystals suitable for X-ray structure analyses were obtained by slow diffusion of diethyl ether in an acetone solution of [**4**][O_3SCF_3]$_6$.

[Ru$_3$(η^6-*p*-Pr^{i}C$_6$H$_4$Me)$_3$(μ_3-3-tpt-κN)Cl$_6$] (5). A mixture of [Ru(η^6-*p*-Pr^{i}C$_6$H$_4$Me)(μ-Cl)Cl]$_2$ (123 mg, 0.200 mmol) and 3-tpt (42 mg, 0.133 mmol) was suspended in CH_2Cl_2 (20 mL) and stirred for 3 h at 40 °C. The volume was reduced to 5 mL, and the orange-red solid was precipitated by addition of diethyl ether, filtered, and dried under vacuum (yield 85 mg, 52%). ^{1}H NMR (400 MHz, CD_2Cl_2): δ (ppm) 10.46 (s, 3H, H$_\delta$), 9.34 (d, 3H, ^3J = 5.48 Hz, H$_\alpha$), 9.09 (d, 3H, ^3J = 8.08 Hz, H$_\gamma$), 7.67 (dd, 3H, H$_\beta$), 5.77 (d, 6H, ^3J = 6.04 Hz, Ar$_{p-cym}$), 5.53 (d, 6H, Ar$_{p-cym}$), 3.07 (sep, 3H, ^3J = 6.92 Hz, C*H*(CH$_3$)$_2$), 2.08 (s, 9H, CH$_3$), 1.41 (d, 18H, CH(C*H*$_3$)$_2$). ^{13}C{^{1}H} NMR (100 MHz, CD_2Cl_2): δ (ppm) 170.1, 158.6, 156.4, 138.0, 132.0, 125.1, 103.4, 97.7, 84.3, 82.4, 31.3, 22.5, 18.5. IR (cm^{-1}): 1525 (s), 1369 (s), 803 (s). Anal. Calcd for $C_{48}H_{54}N_6Cl_6Ru_3$: C, 46.83; H, 4.42; N, 6.82. Found: C, 46.91; H, 4.42; N, 6.63.

[Ru$_3$(η^6-C$_6$Me$_6$)$_3$(μ_3-3-tpt-κN)Cl$_6$] (6). A mixture of [Ru(η^6-C$_6$Me$_6$)(μ-Cl)Cl]$_2$ (167 mg, 0.25 mmol) and 3-tpt (52 mg, 0.17 mmol) was suspended in CH_2Cl_2 (20 mL) and stirred for 3 h at 40 °C. The volume was reduced to 5 mL, and the orange-red solid was precipitated by addition of diethyl ether and filtered (yield 170 mg, 77%). ^{1}H NMR (400 MHz, $CDCl_3$): δ (ppm) 10.06 (s, 3H, H$_\delta$), 9.13 (d, 3H, ^3J = 4.04 Hz, H$_\alpha$), 8.94 (d, 3H, H$_\gamma$), 7.60 (br, 3H, H$_\beta$), 2.08 (s, 54H, CH$_3$). ^{13}C{^{1}H} NMR (100 MHz, $CDCl_3$): δ (ppm) 170.4, 158.5, 155.9, 137.8, 132.3, 125.2, 92.0, 16.0. IR

Table 2. Crystallographic and Selected Experimental Data For [3][O_3SCF_3]$_6$·$(CH_3)_2CO$, [4][O_3SCF_3]$_6$, and [8][O_3SCF_3]$_6$

	[**3**][O_3SCF_3]$_6$·$(CH_3)_2CO$	[**4**][O_3SCF_3]$_6$	[**8**][O_3SCF_3]$_6$
chem formula	$C_{105}H_{114}Cl_6F_{18}N_{12}O_{19}Ru_6S_6$	$C_{114}H_{132}Cl_6F_{18}N_{12}O_{18}Ru_6S_6$	$C_{114}H_{132}Cl_6F_{18}N_{12}O_{18}Ru_6S_6$
formula wt	3201.56	3311.80	3311.80
cryst syst	monoclinic	monoclinic	monoclinic
space group	*C*2/*c*	$P2_1/n$	$P2_1/n$
cryst color and shape	orange plate	orange plate	orange plate
cryst size	0.49 × 0.28 × 0.17	0.48 × 0.15 × 0.10	0.24 × 0.18 × 0.07
a (Å)	76.294(6)	23.8695(14)	13.1582(7)
b (Å)	18.2792(11)	17.2330(8)	32.575(2)
c (Å)	19.1459(10)	35.282(2)	33.7963(14)
β (deg)	94.152(7)	93.499(7)	97.394(4)
V (Å^3)	26 631(3)	14 485.9(14)	14 365.6(12)
Z	8	4	4
T (K)	203(2)	203(2)	173(2)
D_c (g cm^{-3})	1.597	1.519	1.531
μ (mm^{-1})	0.966	0.890	0.898
scan range (deg)	4.18 < 2θ < 51.90	4.00 < 2θ < 51.94	2.50 < 2θ < 50.62
no. of unique rflns	25 133	28 107	25 651
no. of rflns used ($I > 2\sigma(I)$)	14 128	12 233	13 751
R_{int}	0.0625	0.0738	0.0918
final R1, wR2 indices ($I > 2\sigma(I)$)[a]	0.0546, 0.1390	0.0510, 0.1188	0.0584, 0.1127
R1, wR2 indices (all data)	0.1016, 0.1537	0.1069, 0.1321	0.1284, 0.1346
goodness of fit	0.902	0.749	0.911
max, min $\Delta\rho$ (e Å^{-3})	1.887, −3.162	0.601, −0.912	0.677, −1.292

[a] Structures were refined on F_o^2: wR2 = $[\sum[w(F_o^2 - F_c^2)^2]/\sum w(F_o^2)^2]^{1/2}$, where $w^{-1} = [\sum(F_o^2) + (aP)^2 + bP]$ and $P = [\max(F_o^2, 0) + 2F_c^2]/3$.

(cm^{-1}): 1523 (s), 1367 (s), 805 (s). Anal. Calcd for $C_{54}H_{66}N_6Cl_6Ru_3$: C, 49.32; H, 5.06; N, 6.39. Found: C, 49.75; H, 5.38; N, 6.31.

[Ru_6(η^6-*p*-Pr^iC_6H_4Me)$_6$(μ_3-3-tpt-κN)$_2$(μ-Cl)$_6$][O_3SCF_3]$_6$ ([7][O_3SCF_3]$_6$). A mixture of **5** (60 mg, 0.05 mmol) and Ag(O_3SCF_3) (38 mg, 0.15 mmol) in acetone (20 mL) was stirred at room temperature for 4 h and then filtered. The filtrate was concentrated (3 mL), and diethyl ether was slowly added to precipitate an orange solid (yield 50 mg, 65%). ^{1}H NMR (200 MHz, acetone-d_6): δ (ppm) = 9.67 (d, 6H, ^4J = 1.60 Hz, H_δ) (▲), 9.64 (d, 4H, ^4J = 1.60 Hz, H_δ) (●), 9.57 (d, 2H, ^4J = 1.60 Hz, H_δ) (●), 9.28 (dd, 2H, H_γ) (●), 9.23 (dd, 2H, H_γ) (●), 8.89−8.82 (m, 20H, H_γ, H_α) (●▲), 7.84−7.65 (m, 12H, H_β) (●▲), 6.44−6.37 (m, 12H, Ar_{p-cym}), 6.34−623 (m, 12H, Ar_{p-cym}), 6.20−6.17 (m, 12H, Ar_{p-cym}), 6.07−5.91 (m, 12H, Ar_{p-cym}), 3.17−2.99 (m, 12H, C*H*(CH_3)$_2$), 2.49 (s, 18H, CH_3), 2.36 (s, 18H, CH_3), 1.54−1.36 (m, 72H, CH(C*H*$_3$)$_2$). ^{13}C-{^{1}H} NMR (100 MHz, acetone-d_6): δ (ppm) 170.1, 169.3, 168.9, 159.2, 156.9, 154.5, 141.2, 139.4, 134.1, 132.1, 127.6, 123.3, 120.1, 106.0, 103.8, 103.4, 99.5, 99.2, 85.4, 83.7, 83.3, 81.6, 31.2, 31.1, 22.2, 21.5, 19.0, 17.6, 17.5. IR (cm^{-1}): 1525 (s), 1369 (s), 803 (s). Anal. Calcd for $C_{102}H_{108}N_{12}Cl_6O_{18}S_6F_{18}Ru_6$: C, 38.97; H, 3.46; N, 5.34. Found: C, 38.65; N, 3.37; N, 5.22.

[Ru_6(η^6-C_6Me_6)$_6$(μ_3-3-tpt-κN)$_2$(μ-Cl)$_6$][O_3SCF_3]$_6$ ([8][O_3SCF_3]$_6$). A mixture of **6** (120 mg, 0.091 mmol) and Ag(O_3SCF_3) (70 mg, 0.27 mmol) in CH_2Cl_2 (20 mL) was stirred at 50 °C for 4 h and then filtered. The filtrate was concentrated (3 mL), and diethyl ether was slowly added to precipitate an orange solid (yield 120 mg, 79%). ^{1}H NMR (400 MHz, acetone-d_6): δ (ppm) 9.51 (d, 6H, ^4J = 1.94 Hz, H_δ), 8.85 (dd, 6H, ^3J = 4.60 Hz, H_α), 8.69 (d, 6H, ^3J = 5.64 Hz, H_γ), 7.99 (dd, 6H, H_β), 2.22 (s, 108H, C_6Me_6). ^{13}C-{^{1}H} NMR (100 MHz, acetone-d_6): δ (ppm) 169.1, 158.9, 154.1, 139.8, 132.6, 129.0, 94.0, 15.5. IR (cm^{-1}): 1636 (s), 1531 (s), 1384 (s), 1260 (s), 1161 (s), 1032 (s), 639 (s). Anal. Calcd for $C_{114}H_{132}N_{12}Cl_6O_{18}S_6F_{18}Ru_6$: C, 41.34; H, 4.01; N, 5.07. Found: C, 41.80; H, 3.95; N, 5.05.

Crystals suitable for X-ray structure analyses were obtained by slow diffusion of diethyl ether in an acetone solution of [**8**][O_3SCF_3]$_6$.

X-ray Crystallographic Study. Crystals of [Ru_6(η^6-*p*-Pr^iC_6H_4Me)$_6$(μ_3-4-tpt-κN)$_2$(μ-Cl)$_6$][O_3SCF_3]$_6$·$(CH_3)_2CO$ ([**3**][O_3SCF_3]$_6$) and [Ru_6(η^6-C_6Me_6)$_6$(μ_3-4-tpt-κN)$_2$(μ-Cl)$_6$][O_3SCF_3]$_6$ ([**4**][O_3SCF_3]$_6$) were mounted on a Stoe image plate diffraction system equipped with a ϕ circle goniometer, using Mo Kα graphite-monochromated radiation (λ = 0.710 73 Å) with ϕ range of 0−200°, increments of 0.7 and 0.6°, respectively, a 2θ range from 4.0 to 52°, and $D_{max}-D_{min}$ = 12.45−0.81 Å. A crystal of [Ru_6(η^6-C_6Me_6)$_6$(μ_3-3-tpt-κN)$_2$(μ-Cl)$_6$][O_3SCF_3]$_6$ ([**8**][O_3SCF_3]$_6$) was mounted on a Stoe Mark II image plate diffraction system, using Mo Kα graphite-monochromated radiation, an image plate distance of 135 mm, a 2θ range from 1.7 to 51.6°, and $D_{max}-D_{min}$ = 23.99−0.82 Å. The structures were solved by direct methods using the program SHELXS-97.[26] Refinement and all further calculations were carried out using SHELXL-97.[27] In all cases, the H atoms were included in calculated positions and treated as riding atoms using the SHELXL default parameters. Examination of the structures with PLATON[28] reveals in [**3**][O_3SCF_3]$_6$, [**4**][O_3SCF_3]$_6$, and [**8**][O_3SCF_3]$_6$ voids between the anions and cations. Indeed, in [**3**][O_3SCF_3]$_6$, one molecule of acetone could be refined, but more voids were observed. Similarly in [**4**][O_3SCF_3]$_6$ and [**8**][O_3SCF_3]$_6$, voids corresponding to solvent molecules and disordered triflate molecules were found. Therefore, new data sets corresponding to omission of the missing solvent and anions were generated with the SQUEEZE algorithm[29] and the three structures were refined to convergence. In some cases, disordered triflate anions were modeled and fixed at their position while the well-defined anions were refined anisotropically. However, in all cases the non-H atoms of the prismatic cations were refined anisotropically, using weighted full-matrix least squares on F^2. The remaining positive or negative electron densities greater than 1 e Å^{-3} were all located next to disordered sulfur atoms. Crystallographic details are summarized in Table 2. Figures 2, 3, and 6 were drawn with ORTEP,[30] while Figures 4, 7, and 8 were drawn with MERCURY.[31]

The files CCDC-600474 (for [Ru_6(η^6-*p*-Pr^iC_6H_4Me)$_6$(μ_3-4-tpt-κN)$_2$(μ-Cl)$_6$][O_3SCF_3]$_6$·$(CH_3)_2CO$), CCDC-600475 (for [Ru_6(η^6-C_6Me_6)$_6$(μ_3-4-tpt-κN)$_2$(μ-Cl)$_6$][O_3SCF_3]$_6$), and CCDC-619336 (for [Ru_6(η^6-C_6Me_6)$_6$(μ_3-3-tpt-κN)$_2$(μ-Cl)$_6$][O_3SCF_3]$_6$) contain the supplementary crystallographic data for this paper. These data can be

(26) Sheldrick, G. M. *Acta Crystallogr.* **1990**, *A46*, 467−473.
(27) Sheldrick, G. M. SHELXL-97; University of Göttingen, Göttingen, Germany, 1999.
(28) Spek, A. L. *J. Appl. Crystallogr.* **2003**, *36*, 7−13.
(29) van der Sluis, P.; Spek, A. L. *Acta Crystallogr.* **1990**, *A46*, 194−201.
(30) Farrugia, L. J. *J. Appl. Crystallogr.* **1997**, *30*, 565.
(31) Bruno, I. J.; Cole, J. C.; Edgington, P. R.; Kessler, M.; Macrae, C. F.; McCabe, P.; Pearson, J.; Taylor, R. *Acta Crystallogr.* **2002**, *B58*, 389−397.

obtained free of charge at www.ccdc.cam.ac.uk/conts/retrieving.html (or from the Cambridge Crystallographic Data Centre, 12, Union Road, Cambridge CB2 1EZ, U.K.; fax, (internat.) +44-1223/336-033; e-mail, deposit@ccdc.cam.ac.uk).

Acknowledgment. P.G. acknowledges financial support from the Swiss Federal Commission for Scholarship (FCS). We thank Professor H. Stoeckli-Evans for access to X-ray facilities and Johnson Matthey Research Centre for a generous loan of ruthenium chloride hydrate.

Supporting Information Available: Figures giving selected ^{1}H NMR spectra and CIF files giving X-ray data for **3**, **4**, and **8**. This material is available free of charge via the Internet at http://pubs.acs.org.

OM060843K